

## Design and Application of Lipophilic Nucleosides as Building Blocks to Obtain Highly Functional Biological Surfaces

Holger A. Scheidt,<sup>†</sup> Wolfgang Flasche,<sup>‡</sup> Crina Cismas,<sup>‡</sup> Maximilian Rost,<sup>§</sup> Andreas Herrmann,<sup>§</sup> Jürgen Liebscher,<sup>\*,‡</sup> and Daniel Huster<sup>\*,†,||</sup>

*Junior Research Group "Solid-state NMR Studies of the Structure of Membrane-associated Proteins", Biotechnological-Biomedical Center, University of Leipzig, Liebigstr. 27, D-04103 Leipzig, Germany, Institute of Chemistry, Humboldt-University Berlin, Brook-Taylor-Str. 2, D-12489 Berlin, Germany, Institute of Biology/Biophysics, Humboldt-University Berlin, Invalidenstr. 42, D-10115 Berlin, Germany, and Institute of Medical Physics and Biophysics, University of Leipzig, Liebigstr. 27, D-04103 Leipzig, Germany.*

Received: July 29, 2004

For the potential application in nanobiotechnology, we have synthesized three different lipophilic nucleosides and investigated their membrane insertion and localization by solid-state NMR spectroscopy. The hydrophilic headgroups of these nucleosides consist of an adenine or uracil nucleobase, which is attached to a ribose or deoxyribose moiety. The membrane affinity of these molecules is either achieved by the covalent attachment of a 1-octadecynyl chain or an ethisterol moiety. For the first time, the orientation of these molecules and the quantitative localization of their functional groups are measured. All investigated lipophilic nucleosides can be incorporated into phospholipid membranes at high concentration without destroying the lamellar bilayer structure as shown by <sup>31</sup>P NMR and <sup>2</sup>H NMR. However, the membrane incorporation of the lipophilic nucleosides leads to modifications in the phospholipid packing properties as revealed by <sup>2</sup>H NMR on chain-deuterated phospholipids. Although the two nucleosides with the octadecynyl membrane anchor only impose a rather moderate decrease in phospholipid packing density, the nucleoside with a steroid membrane anchor significantly disturbs the lateral organization of the phospholipids in the membrane. Quantitative <sup>1</sup>H nuclear Overhauser enhancement spectroscopy under magic angle spinning conditions has been applied to localize the monosaccharide/nucleobase moiety of the nucleoside in the membrane. This method measures the intermolecular interaction strength between molecular segments. For all molecules, a location of the (deoxy)-ribose/nucleobase moiety in the lipid–water interface of the membrane has been found that exposes the nucleobase to the aqueous phase, where an interaction with external molecular patterns could take place. These molecules may be useful building blocks to obtain a functionalized membrane surface that can be recognized by complementary nucleic acid strands.

### Introduction

In millions of years of evolution, nature has developed highly specific biological recognition patterns based on the molecular binding of polymeric nucleobase structures via hydrogen bonds. These molecular building blocks are assembled into highly specific DNA or RNA structures of large molecular weight that contain tremendous amounts of information. By these molecular structures, genetic information is stored and replicated. In recent years, biochemical DNA-based recognition principles have also been used for the development of macroscopic functional materials.<sup>1–3</sup> These materials have been assembled from nucleobases and inorganic building blocks that are rationally designed to recognize binding partners in the self-assembly process. These and other innovations have led to the constitution of the new field of nanobiotechnology.<sup>4–6</sup>

DNA-based recognition patterns have also been exploited to build organic self-assembled structures, fibers, films, and other three-dimensional shapes.<sup>7–13</sup> In particular, membranes represent interesting structures for the development of highly functional surfaces. Phospholipid membranes are versatile structures that can be formed by many different lipid molecules and can accommodate or bind a large number of molecular species. For instance, supported lipid bilayers have been doped with phospholipid molecules that display a covalently bound short, single-stranded DNA molecule. Next, vesicles displaying antisense oligonucleotides are tethered to the membrane by a self-assembly process.<sup>7</sup> In principle, all kinds of molecules such as enzymes, pharmacological drugs, fluorescence probes, or electrically conducting building blocks could be specifically bound to lipid surfaces by such DNA-based recognition and binding mechanisms to obtain highly functional surfaces.

Various lipophilic groups can be attached to oligonucleotides providing a membrane anchor.<sup>14–17</sup> Hydrophobic membrane anchors are also often encountered in biology. For instance, many proteins involved in signal transduction are lipidated.<sup>18</sup> This provides the soluble protein molecules with hydrophobic energy that attaches them to the membrane surface. Thus, their effective concentration is increased by orders of magnitude, and

\* Corresponding authors. Phone: +49 (0) 341-97-15706 (D.H.), +49 (0) 30-2093-7550 (J.L.). Fax: +49 (0) 341-97-15709 (D.H.), +49 (0) 30-2093-7552 (J.L.). E-mail: huserd@medizin.uni-leipzig.de (D.H.), liebscher@rz.hu-berlin.de (J.L.).

<sup>†</sup> Biotechnological-Biomedical Center.

<sup>‡</sup> Institute of Chemistry.

<sup>§</sup> Institute of Biology/Biophysics.

<sup>||</sup> Institute of Medical Physics and Biophysics.

the probability to interact with downstream effectors raises drastically.<sup>19</sup>

In this paper, lipid modification is employed to synthesize nucleosides with a high membrane affinity. In contrast to the phospholipid-attached oligonucleotides<sup>7</sup> or nucleosides,<sup>10,20</sup> which have been shown to induce hemifusion in giant vesicles<sup>21</sup> or induce vesicle adhesion,<sup>20,22</sup> or can serve as mobile linkers in tethering vesicles on supported lipid bilayers,<sup>7</sup> we have synthesized lipophilic molecules that consist of a single nucleoside and a lipophilic group, such as long alkynyl chains or the steroidal substituents, which are covalently attached to the nucleobase. Such lipophilic nucleosides will allow formation of oligonucleotides later on via the 3'- and 5'-positions. Thus, the weak interactions between the membrane-attached nucleosides and the complementary DNA or RNA patterns can be amplified. The lipophilic nucleosides should be easily incorporated into lipid membranes, on one hand, and could bind to complementary single-stranded DNA molecules that could carry an enzyme or other molecules of interest, on the other hand. Thus, versatile lipophilic nucleosides can be combined to bind a number of different targets to the membrane to obtain highly functional surfaces.

A large number of molecular combinations of nucleobases with lipophilic groups is possible. Out of the configurational space, those molecules have to be selected that exhibit three essential properties: (i) The nucleobase has to be exposed to the aqueous phase, (ii) the molecules have to insert permanently into the lipid bilayer, and (iii) the inserted nucleotides should not significantly modify the bilayer structure or induce the formation of nonlamellar phases.

In this paper, we have used solid-state NMR spectroscopy to investigate the membrane incorporation of three lipophilic nucleosides **1**, **2**, and **3** (see Figure 1). The hydrophilic headgroups of these nucleoside molecules consist of an adenine or uracil nucleobase, which is attached to a ribose or deoxyribose moiety. The membrane affinity of these molecules (**1**, **2**, and **3**) is either achieved by the covalent attachment of a 1-octadecynyl chain or the ethisterone moiety. These molecules have been incorporated into the phosphatidylcholine model membranes at a molar concentration of 20 mol %.

The phase state of the host membrane after incorporation of the lipophilic nucleosides is investigated by <sup>31</sup>P NMR, which is highly sensitive to the observation of nonlamellar phases of disrupted bilayers.<sup>23</sup> Phospholipid headgroup orientation and the packing density in the membrane are investigated by <sup>2</sup>H NMR methods.<sup>24–26</sup> Finally, the localization of the functional groups in the membrane was determined by measurements of intermolecular cross-relaxation rates by <sup>1</sup>H magic angle spinning (MAS) nuclear Overhauser enhancement spectroscopy (NOESY).<sup>27</sup>

These methods allow an assessment of the usefulness of these molecules to build highly functional membrane surfaces.

## Materials and Methods

**Materials.** 1-Palmitoyl-2-oleoyl-*sn*-glycero-3-phosphocholine (POPC), 1-palmitoyl-*d*<sub>31</sub>-2-oleoyl-*sn*-glycero-3-phosphocholine (POPC-*d*<sub>31</sub>), 1,2-dimyristoyl-*d*<sub>54</sub>-*sn*-glycerol-3-phosphocholine-1,1,2,2-*d*<sub>4</sub>-*N,N,N*-trimethyl-*d*<sub>9</sub> (DMPC-*d*<sub>67</sub>), and 1,2-dimyristoyl-*sn*-glycero-3-phosphocholine-1,1,2,2-*d*<sub>4</sub> (DMPC-*d*<sub>4</sub>) were purchased from Avanti Polar Lipids, Inc. (Alabaster, AL) and used without further purification.

**Synthesis of Lipophilic Nucleosides. 8-(Octadec-1-yn-1-yl)-adenosine 1.** Octadecan-1-yne (1.50 g, 6.00 mmol) was added to a degassed solution of 8-bromoadenosine (330 mg, 1.00

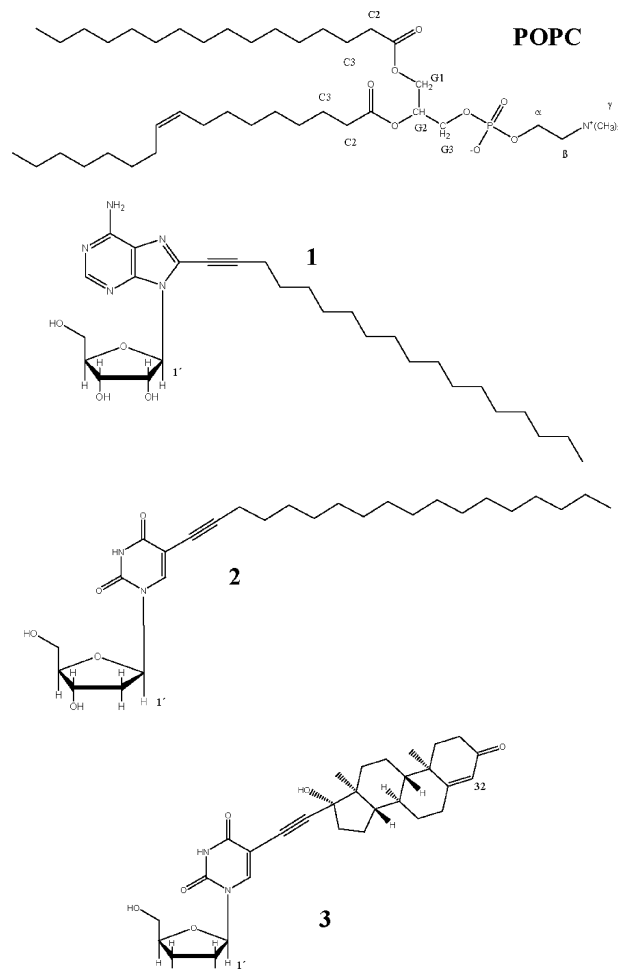


**Figure 1.** Chemical structure of POPC and the investigated lipophilic nucleosides **1**, **2**, and **3**. The hydrogen atoms used for the determination of intermolecular cross-relaxation rates to the phospholipid membrane in <sup>1</sup>H NOESY experiments are marked with numbers.

mmol) in dry DMF (29.5 mL) and Et<sub>3</sub>N (4.5 mL) under stirring and a constant stream of argon. After 5 min, Pd(PPh<sub>3</sub>)<sub>2</sub>Cl<sub>2</sub> (17 mg, 0.024 mmol) and CuI (1 mg, 0.005 mmol) were added, and the solution was kept at room temperature for 4 h. After the reaction was finished (TLC), the solid was filtered off and recrystallized from EtOH/Et<sub>2</sub>O to give 0.425 g (82%) of the product as a slightly brownish solid. mp 134–138 °C (CH<sub>2</sub>-Cl<sub>2</sub>/EtOH). <sup>1</sup>H NMR δ, *J* (Hz), (DMSO-*d*<sub>6</sub>): 0.90 (t, 3H, 6.03 Hz, CH<sub>3</sub>), 1.28 (m, 24H, (CH<sub>2</sub>)<sub>12</sub>), 1.48 (m, 2H, CH<sub>2</sub>), 1.64 (m, 2H, CH<sub>2</sub>), 2.62 (t, 2H, 6.78 Hz, CH<sub>2</sub>), 3.59 (m, 1H, H-5'a), 3.73 (m, 1H, H-5'b), 4.03 (m, 1H, H-4'), 4.24 (m, 1H, H-3'), 5.05 (dd, 1H, 6.03, 11.85 Hz, H-2'), 5.23 (d, 1H, 4.14 Hz, OH-3'), 5.45 (d, 1H, 6.42 Hz, OH-2'), 5.62 (dd, 1H, 3.75, 8.67 Hz, OH-5'), 5.98 (d, 1H, 6.78 Hz, H-1'), 7.62 (br s, 2H, NH<sub>2</sub>), 8.20 (s, 1H, adenine H-2). <sup>13</sup>C NMR δ (DMSO-*d*<sub>6</sub>): 14.05 (CH<sub>3</sub>), 18.66 (CH<sub>2</sub>-C≡C), 22.19–31.39 (alkyl CH<sub>2</sub>), 62.32 (C-5'), 70.28 (C<sub>q</sub>), 71.10 (C-3'), 71.56 (C-2'), 86.64 (C-4'), 89.38 (C-1'), 97.60, 134.12, 146.91, 156 (C<sub>q</sub>), 153.07 (adenine, C-2). HRMS (ESI) *m/z*: Calcd for C<sub>28</sub>H<sub>46</sub>N<sub>5</sub>O<sub>4</sub> 516.3544, found 516.3545.

**5-(1-Octadecynyl)-2'-deoxyuridine 2.** Octadecan-1-yne (0.71 g, 2.8 mmol) was added to a degassed solution of 5-iodo-2'-deoxyuridine (1.00 g, 2.825 mmol) in dry DMF (10 mL) and dry ethyldiisopropylamine (730 mg, 1.00 mL, 5.65 mmol) under stirring and a constant stream of argon. After 5 min, Pd(PPh<sub>3</sub>)<sub>4</sub> (327 mg, 0.28 mmol) and CuI (108 mg, 0.57 mmol) were added, and the solution was kept at room temperature for 48 h. After

the reaction was finished (TLC), the solvents were removed under reduced pressure. The residue was purified by column chromatography,  $R_f$  0.28 (CH<sub>2</sub>Cl<sub>2</sub>/MeOH 95/5), to give 0.37 g (0.78 mmol, 28%) of a colorless solid. mp 206–208 °C (MeOH) under decomposition. <sup>1</sup>H NMR  $\delta$ ,  $J$  (Hz), (CD<sub>3</sub>OD): 1.00 (s, 3H, CH<sub>3</sub>), 1.39–1.63 (m, br, 26 H, CH<sub>2</sub>), 2.26 (m, br 2H, CH<sub>2</sub>), 3.51 (s, br, 2H, CH<sub>2</sub>), 3.75 (s, br, 1H, CH), 3.95 (s, br, 1H, CH), 4.39 (s, b, 1H, CH), 5.29 (s, br, 1H, HO), 5.32 (s, b, 1H, HO), 6.27 (s, b, 1H, CH), 8.56 (s, 1H, CH), 11.70–11.82 (s, br, NH). <sup>13</sup>C NMR  $\delta$  (CD<sub>3</sub>OD): 14.0 (CH<sub>3</sub>), 18.9 (CH<sub>2</sub>), 22.2 (CH<sub>2</sub>), 28.3–29.2 (CH<sub>2</sub> 12C), 31.4 (CH<sub>2</sub>), 40.4 (CH<sub>2</sub>), 60.9 (CH<sub>2</sub>), 69.4 (CH), 70.3 (CH), 84.7 (CH), 87.6 (CH), 93.3 (C), 99.2 (C), 145.1 (CH), 150.2 (C), 160.6 (NH–C). HRMS (ESI)  $m/z$ : Calcd for C<sub>27</sub>H<sub>45</sub>O<sub>5</sub>N<sub>2</sub> 477.3323, found 477.3305.

5-[2-(16-Hydroxy-10,13-dimethyl-3-oxo-2,3,6,7,8,9,10,11,12-, 13,14,15,16,17-tetradecahydro-1H-cyclopenta[a]phenanthren-16-yl)ethynyl]-2,4-(1H,3H)-uridine 3.<sup>28</sup> Ethisterone (0.92 g, 3.00 mmol) was added to a solution of 5-iodouridine (1.00 g, 2.70 mmol) and dry *i*-Pr<sub>2</sub>NEt (1 mL, 5.65 mmol) in dry DMF (10 mL) under argon. After the addition of Pd(PPh<sub>3</sub>)<sub>4</sub> (327 mg, 0.28 mmol) and CuI (108 mg, 0.57 mmol), the solution was stirred at room temperature until all starting material had disappeared (TLC, about 48 h). Silica gel (~1 g) was added to the solution, and the DMF was removed under reduced pressure. The remaining silica gel was transferred to a chromatography column filled with silica gel, followed by flash chromatography using a gradient with 500 mL of each solvent (mixture) (Hexan → Hexan/CHCl<sub>3</sub> 5/1 → 3/1 → 1/1 → 1/3 → CHCl<sub>3</sub> → CHCl<sub>3</sub>/MeOH 9/1). The product was obtained as a white powder in the chloroform fraction at 1.73 g (2.70 mmol, 100%). mp 125–130 °C (CHCl<sub>3</sub>/MeOH 100/1). <sup>1</sup>H NMR  $\delta$ ,  $J$  (Hz) (DMSO-*d*<sub>6</sub>): 1.09 (s, br, CH), 1.41 (s, 3H, CH<sub>3</sub>), 1.60 (s, 3H, CH<sub>3</sub>), 1.63–2.67 (m, 18H, CH<sub>2</sub>), 3.45 (q, 2H,  $J$  = 7.17, CH<sub>2</sub>), 3.56 (s, 2H, CH<sub>2</sub>), 4.27 (m, 1H, CH), 4.45 (m, 2H, CH<sub>2</sub>), 4.82–5.05 (br, 4H, OH), 5.91 (s, 1H, CH), 6.08 (d, 1H,  $J$  = 3.75 CH), 8.58 (s, 1H, CH). <sup>13</sup>C NMR  $\delta$  (DMSO-*d*<sub>6</sub>): 12.4 (CH<sub>3</sub>), 16.8 (CH<sub>2</sub>), 17.3 (CH<sub>3</sub>), 20.7 (CH<sub>2</sub>), 23.0 (CH<sub>2</sub>), 31.7 (CH<sub>2</sub>), 32.7 (CH), 33.6 (CH<sub>2</sub>), 35.5 (C), 38.8 (CH<sub>2</sub>), 42.9 (CH<sub>2</sub>), 50.1 (CH), 53.6 (CH<sub>2</sub>), 54.7 (CH), 60.8 (CH<sub>2</sub>), 69.7 (CH), 74.6 (CH), 76.6 (CH), 79.7 (C), 85.2 (CH), 89.7 (CH), 97.3 (C), 99.5 (C), 123.0 (C), 143.8 (C), 150.3 (C), 163.2 (C), 174.8 (C), 201.8 (C). HRMS  $m/z$ : Calcd for C<sub>30</sub>H<sub>39</sub>O<sub>8</sub>N<sub>2</sub><sup>+</sup> 555.26990 [M + H]<sup>+</sup>, found 555.26950 [M + H]<sup>+</sup>.

**Sample Preparation.** For the NMR measurements, the phospholipids and the respective nucleosides (molar ratio of 4:1) were codissolved in a chloroform/methanol mixture. After evaporating the solvent, the samples were dissolved in cyclohexane and lyophilized at high vacuum to obtain a fluffy powder. Samples were hydrated with 40 wt % D<sub>2</sub>O for <sup>1</sup>H NMR measurements or with deuterium-depleted H<sub>2</sub>O for <sup>2</sup>H NMR measurements, yielding spherical multilamellar vesicles made of liquid crystalline bilayers above the main phase transition of the phospholipids. For equilibration and to obtain a homogeneous distribution of the lipophilic nucleosides, ten freeze–thawing cycles and gentle centrifugation were applied. For the <sup>1</sup>H MAS NMR experiments, the samples were transferred into 4-mm HR MAS rotors with spherical Kel-F inserts; for static <sup>2</sup>H NMR measurements, samples were transferred into 5-mm glass vials.

**Solution NMR Spectroscopy.** Standard gradient <sup>1</sup>H–<sup>13</sup>C heteronuclear single quantum coherence (HSQC)<sup>29</sup> spectra were acquired in a deuterated chloroform/methanol solution (1:1, v/v) using a Bruker DRX 600 NMR spectrometer (Bruker BioSpin GmbH, Rheinstetten), operating at a resonance frequency of

600.1 MHz for <sup>1</sup>H and 150.9 MHz for <sup>13</sup>C. HSQC spectra were acquired using 90° pulse lengths of 10.7 and 14.5  $\mu$ s for <sup>1</sup>H and <sup>13</sup>C, respectively. All NMR measurements were carried out at a temperature of 303 K.

**Static <sup>2</sup>H and <sup>31</sup>P NMR Spectroscopy.** The static <sup>31</sup>P NMR spectra of membrane samples were acquired on a Bruker DRX 600 NMR spectrometer operating at a resonance frequency of 242.8 MHz for <sup>31</sup>P using a Hahn-echo pulse sequence. A <sup>31</sup>P 90° pulse length of 7  $\mu$ s, a Hahn-echo delay of 50  $\mu$ s, a spectral width of 100 kHz, and a recycle delay of 2 s were used. Continuous-wave proton decoupling was applied during signal acquisition. Spectral simulations of the <sup>31</sup>P NMR line shape were carried out to obtain the chemical shift anisotropy ( $\Delta\sigma$ ) using a program written in *Mathcad 2001* (MathSoft Engineering & Education Inc., Cambridge, MA).

Static <sup>2</sup>H NMR spectra were recorded on a Bruker Avance 400 NMR spectrometer operating at a resonance frequency of 61.2 MHz for <sup>2</sup>H using a double channel solids probe equipped with a 5-mm solenoid coil. The <sup>2</sup>H spectra were accumulated at a spectrum width of 500 kHz using a phase-cycled quadrupolar echo sequence<sup>30</sup> and a relaxation delay of 500 ms. The two 3- $\mu$ s  $\pi/2$  pulses were separated by a 60- $\mu$ s delay.

The <sup>2</sup>H NMR spectra of DMPC-*d*<sub>4</sub> in the presence and absence of lipophilic nucleosides were simulated using the *Mathcad 2001* program to obtain the quadrupolar splitting of the two deuterated methylene groups of the lipid headgroup.

The spectra of the POPC-*d*<sub>31</sub> samples in the presence and absence of the lipophilic nucleosides were de-Paked and analyzed as described in detail in the literature.<sup>31,32</sup> Smoothed chain order parameter profiles were calculated using the reported procedure.<sup>33</sup>

The effective length of a saturated hydrocarbon chain ( $\langle L \rangle$ ) was calculated from the average order parameter ( $\langle S \rangle$ ) according to eq 1<sup>34</sup> where  $l = m \times 1.27$  Å is the length of an all-trans chain

$$\langle L \rangle = l(0.5 + \langle S \rangle) \quad (1)$$

with  $m$  as the number of C–C bonds, and 1.27 Å is the distance between neighboring carbon atoms.

Changes  $\Delta A$  in area per phospholipid molecule caused by the incorporation of lipophilic nucleosides were calculated from the differences in chain length according to eq 2.<sup>35</sup> Here,  $L_1$

$$\Delta A = \frac{V_{\text{Chains}}}{\langle L_1 \rangle \langle L_2 \rangle} (\langle L_1 \rangle - \langle L_2 \rangle) \quad (2)$$

and  $L_2$  are the average phospholipid chain lengths before and after addition of the lipophilic nucleosides. The lipid chain volume,  $V_{\text{Chains}}$ , of POPC was calculated to 861 Å<sup>3</sup> according to the values given in ref 36.

**<sup>1</sup>H MAS NMR Spectroscopy.** <sup>1</sup>H MAS NMR spectra were acquired at a spinning speed of 7 kHz on a Bruker DRX 600 NMR spectrometer using a 4-mm HR MAS probe. Typical  $\pi/2$  pulse lengths were 9  $\mu$ s. A <sup>2</sup>H lock was used for field stability.

Two-dimensional <sup>1</sup>H MAS NOESY spectra<sup>37,38</sup> were acquired at various mixing times (between 1 and 450 ms). The dwell time of the indirect dimension was set equal to one rotor period to avoid folding of spinning sidebands into the centerband region of the 2D NOESY spectra. Typically, between 500 and 600 data points were acquired in the indirect dimension with 16 scans per increment at a relaxation delay between 3.2 and 3.5 s.

The volumes of the respective diagonal and cross-peaks were integrated using the Bruker *XWINNMR* software package. NOE build-up curves were fitted to the spin-pair model yielding cross-relaxation rates ( $\sigma_{ij}$ ) according to eq 3.<sup>39</sup> Here,  $A_{ij}(t_m)$  represents



$$A_{ij}(t_m) = \frac{A_{ij}(0)}{2} [1 - \exp(-2\sigma_{ij}t_m)] \exp\left(-\frac{t_m}{T_{ij}}\right) \quad (3)$$

the cross-peak volume at mixing time  $t_m$ , and  $A_{ij}(0)$  represents the diagonal-peak volume at a mixing time of zero. The value  $1/T_{ij}$  defines a rate of magnetization leakage toward the lattice. Cross-relaxation rates were obtained from the fitting of experimental cross-peak volumes at varying mixing times to eq 3 using the nonlinear regression curve fitter in *ORIGIN* (OriginLab Cooperation, Northampton, MA). To identify intramolecular cross-peaks of the nucleic acid building blocks, NOESY measurements were repeated using a perdeuterated DMPC- $d_{67}$  lipid matrix.

## Results

**Structure of Lipid Membranes in the Presence of Lipophilic Nucleosides.** To study the membrane structure in the presence of lipophilic nucleosides,  $^{31}\text{P}$  and  $^2\text{H}$  NMR measurements were carried out.  $^{31}\text{P}$  NMR spectra of POPC membranes in the presence of the three nucleosides **1**, **2**, and **3** are shown in Figure 2 (left column). These data confirm the presence of the lamellar liquid crystalline lipid phase for all preparations, irrespective of the relatively high content of lipidated nucleosides. From the spectral shape and the anisotropy of chemical shift ( $\Delta\sigma$ ), the influence of these molecules on phospholipid headgroup structure and dynamics can be studied. Both **2** and **3** do not perturb the phospholipid headgroups, as indicated by very similar spectra compared to pure POPC. However, the  $^{31}\text{P}$  NMR spectrum of POPC membranes in the presence of **1** is significantly broadened, indicating a phospholipid headgroup perturbation. Quantitative values for the chemical shift anisotropy, obtained from best-fit simulations (dashed lines in Figure 2), are given in Table 1.

The increase of the  $^{31}\text{P}$  CSA of POPC in the presence of **1** could be due to a change in the headgroup orientation of POPC or its dynamics caused by interactions with the lipophilic nucleosides.<sup>26</sup> Therefore, we further studied the influence of these molecules (**1**, **2**, and **3**) on the headgroup orientation by  $^2\text{H}$  NMR. Because headgroup-deuterated POPC- $d_4$  is not commercially available, we conducted these experiments on DMPC- $d_4$ . In case of a change in the average orientation of the headgroup, characteristic changes of the quadrupolar splittings would be observed.<sup>26</sup>

$^2\text{H}$  NMR spectra of DMPC- $d_4$  in the absence and presence of the nucleobases are shown in Figure 2 (right column). Only a single quadrupolar splitting is resolved in all spectra, indicating that the headgroup orientation of DMPC molecules is only negligibly influenced by the presence of the lipophilic nucleobases. The  $^2\text{H}$  NMR spectra were simulated using a superposition of two Pake doublets to extract the two quadrupolar splittings for the two deuterated methylene groups in the phospholipid headgroup (dashed lines). Results of this analysis are also given in Table 1. All lipophilic nucleosides only moderately influence the headgroup orientation. Similar to the  $^{31}\text{P}$  NMR spectra in the presence of **1**,  $^2\text{H}$  NMR spectra are broadened (see Figure 2).

To study the effect of the incorporation of the various nucleosides on the packing properties in the membranes, the  $^2\text{H}$  NMR spectra of the perdeuterated *sn*-1 chain of POPC molecules were acquired. The  $^2\text{H}$  NMR spectra of deuterated POPC- $d_{31}$  membranes in the absence and presence of nucleosides **1**, **2**, and **3** are shown in Figure 3. Significant alterations in the widths of the quadrupolar splittings for the various nucleosides are observed. Figure 4 shows the chain order

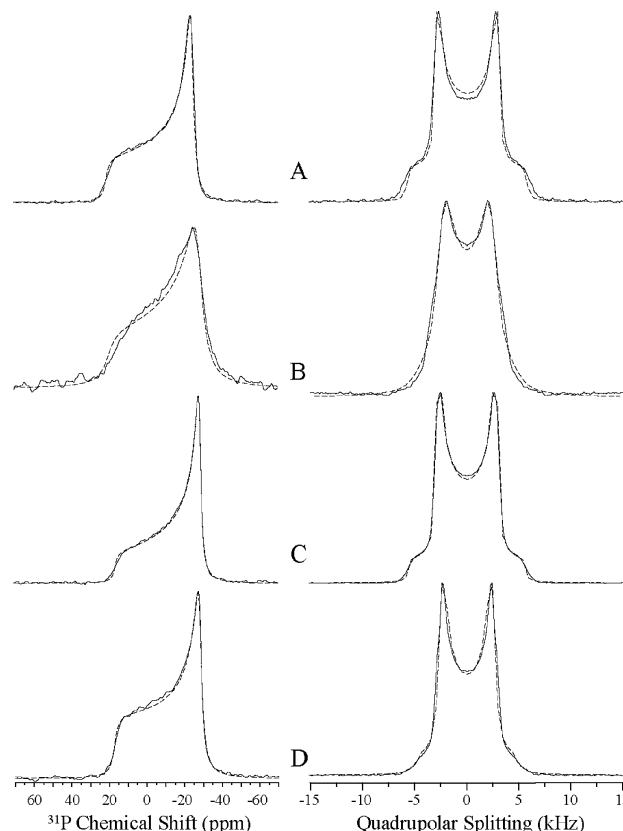


**Figure 2.**  $^{31}\text{P}$  NMR spectra of pure POPC (left) and  $^2\text{H}$  NMR spectra of pure DMPC- $d_4$  membranes (right) (part A); POPC or DMPC- $d_4$  membranes in the presence of 20 mol % of **1** (part B), **2** (part C), and **3** (part D). All measurements were carried out at a water content of 40 wt % and a temperature of 303 K. Dashed lines represent the best-fit simulations of the spectra.

**TABLE 1:  $^{31}\text{P}$  NMR Chemical Shift Anisotropy of POPC and  $^2\text{H}$  Quadrupolar Splitting of DMPC- $d_4$  in the Absence and Presence of 20 mol % of the Lipophilic Nucleosides **1**, **2**, and **3****

	$^{31}\text{P}$ chemical shift anisotropy (ppm)	quadrupolar splitting $\nu_1$ (kHz)	quadrupolar splitting $\nu_2$ (kHz)
pure POPC	45.8		
pure DMPC- $d_4$		5.76	6.1
<b>1</b>	53	4.5	5.4
<b>2</b>	45.0	5.7	5.7
<b>3</b>	45.3	4.7	5.4

parameter profiles as a function of the carbon position and difference order parameter profiles of the POPC membranes.

All nucleosides decrease the chain order of POPC- $d_{31}$  membranes. Molecule **2** induces the smallest alterations of the phospholipid packing density, indicating that the molecules incorporate well into the lipid matrix. The influence of **1** on the lipid chain packing is more pronounced but nevertheless rather moderate. Contrary to these small changes, the POPC chain order is significantly decreased in the presence of **3**, indicating that this molecule largely disturbs phospholipid chain packing.

From chain order parameters, the average length of the phospholipid chains can be calculated. The nucleosides induced a decrease in chain order, which results in a decrease in chain length, which is balanced by an increase in cross-sectional area per POPC molecule. These data are reported in Table 2. For **1** and **2**, small POPC area per molecule changes of less than

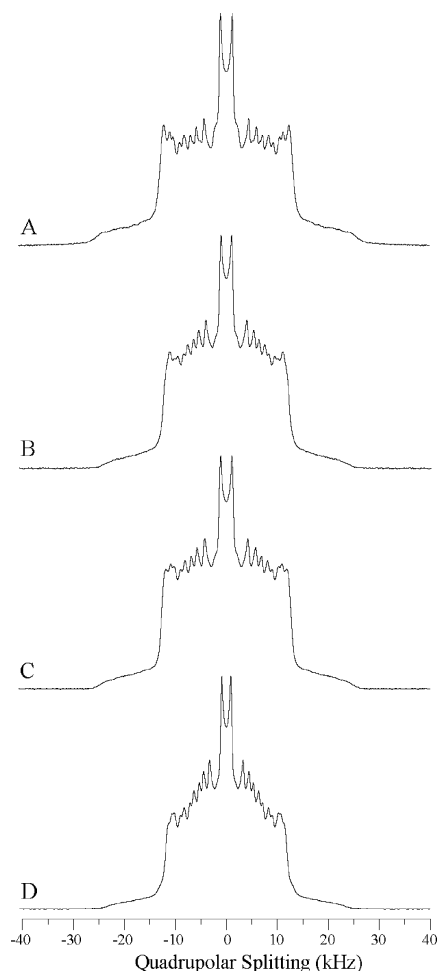


**Figure 3.**  $^2\text{H}$  NMR spectra of pure POPC- $d_{31}$  (part A), **1**/POPC- $d_{31}$  (part B), **2**/POPC- $d_{31}$  (part C), and **3**/POPC- $d_{31}$  mixtures (part D), all at a molar nucleoside/phospholipid mixing ratio of 1:4, water content of 40 wt %, and temperature of 303 K.

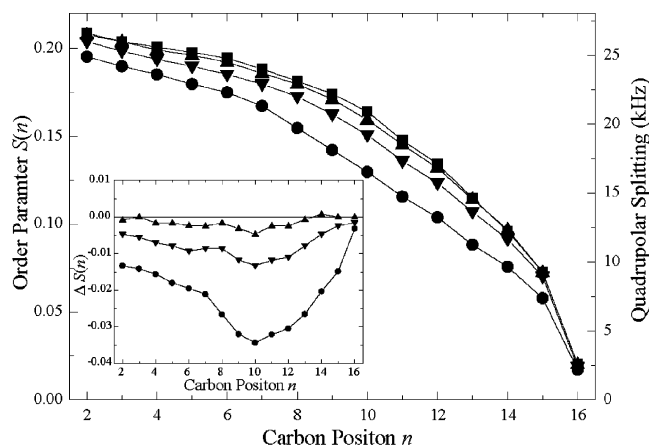


**Figure 4.** Smoothed  $^2\text{H}$  NMR order parameter profiles of the spectra shown in Figure 3 for pure POPC- $d_{31}$  membranes (■) and mixed membranes of **1** and POPC- $d_{31}$  (▼), **2** and POPC- $d_{31}$  (▲), and **3** and POPC- $d_{31}$  (●), all at a molar ratio of 1:4. The inset shows difference order parameter profiles of POPC- $d_{31}$  in the presence of the lipophilic nucleosides with respect to pure POPC- $d_{31}$ .

1  $\text{\AA}^2$  are observed, while incorporation of **3** leads to an area increase of 2.25  $\text{\AA}^2$ .

**Nucleoside–Membrane Interaction Investigated by  $^1\text{H}$  MAS NOESY NMR.** Figure 5 shows the  $^1\text{H}$  MAS NMR spectra of POPC membranes in the presence of the different

**TABLE 2: Average Order Parameter, Average Hydrocarbon Chain Length, and Area Reduction of Pure POPC- $d_{31}$  Membranes in the Absence and Presence of 20 mol % of the Three Lipophilic Nucleosides**

	POPC- $d_{31}$ average order parameter	average chain length ( $\text{\AA}$ )	area increase ( $\text{\AA}^2$ )
pure POPC- $d_{31}$	0.155	13.31	
<b>1</b>	0.148	13.17	0.70
<b>2</b>	0.154	13.29	0.10
<b>3</b>	0.133	12.86	2.25

lipophilic nucleosides **1**, **2**, and **3**. The assignments of the  $^1\text{H}$  signals were obtained by  $^1\text{H}$ – $^{13}\text{C}$  HSQC measurements in an organic solvent. In the membrane environment, small variations of the chemical shifts compared to those in a chloroform/methanol solution occur, indicating the incorporation of the nucleosides into the lipid membranes. Comparison of the integrated signal intensities of the nucleosides and the phospholipids indicates an approximate correspondence with the 1:4 molar ratio of the initial preparation. This shows that the lipophilic nucleosides are fully incorporated into the membrane and are well mixed with the phospholipids. There are no indications for a phase separation between the two components of the mixture. Nevertheless, it has to be considered that the signal intensities of  $^1\text{H}$  MAS spectra are not precisely proportional to the number of protons. This is caused by spinning sidebands of varying intensity according to the residual dipolar couplings of the molecular segments.<sup>40</sup>

The  $^1\text{H}$  MAS NMR spectra of Figure 5 are dominated by the signals from POPC. Methylene and methyl groups from the lipid anchor are superimposed with the signals from the phospholipid acyl chains at  $\sim 0.9$ – $2.5$  ppm, as confirmed by the  $^1\text{H}$  MAS NMR measurements of the lipophilic nucleosides in perdeuterated DMPC- $d_{67}$  (spectra not shown). Similarly, the signals from the steroidal core of **3** are superimposed with the aliphatic DMPC- $d_{67}$  signals. Most resonances from the ribose or deoxyribose are superimposed with the headgroup (i.e., the glycerol signals of the phospholipids and the residual water signal at  $\sim 3.0$ – $5.5$  ppm). However, for each lipophilic nucleoside, a few characteristic signals can be resolved and assigned.

For **1**, the methylene group next to the triple bond in the chain (propargylic  $\text{CH}_2$ ) at 2.6 ppm and the  $1'$  CH signal of the ribose at 6.1 ppm can be resolved (Figure 5 A). The signal at the 2-position of the adenine could not be resolved in the membrane environment, even though it is present in an organic solution. If the spectrum is scaled drastically (Figure 5A), additional broad signals appear; however, it is not clear if these are related to the adenine H2 signal or residual OH and NH groups broadened by the fast exchange.

For **2** and **3**, signals from the  $1'$  H-atom at the (deoxy)ribose and the H-atom at the 6-position of the uracil ring are resolved (Figure 5B,C). In addition, an H-atom at position 32 on the steroid is resolved at 5.6 ppm.

To investigate the location and orientation of the lipophilic nucleosides in lipid membranes,  $^1\text{H}$  NOESY MAS experiments have been carried out. Figure 6 shows the downfield region of the NOESY spectrum of **3**/POPC (1:4 molar ratio) at a mixing time of 300 ms. All resolved signals of the lipophilic nucleoside show intermolecular cross-peaks with lipid signals confirming the good incorporation of these molecules into the phospholipid matrix. The cross-peak volume provides a measurement of the interaction strength between the protons of interacting molecular segments. Therefore, the quantitative analysis of the cross-relaxation rates provides information about the contact probability of the respective protons.<sup>40–42</sup>

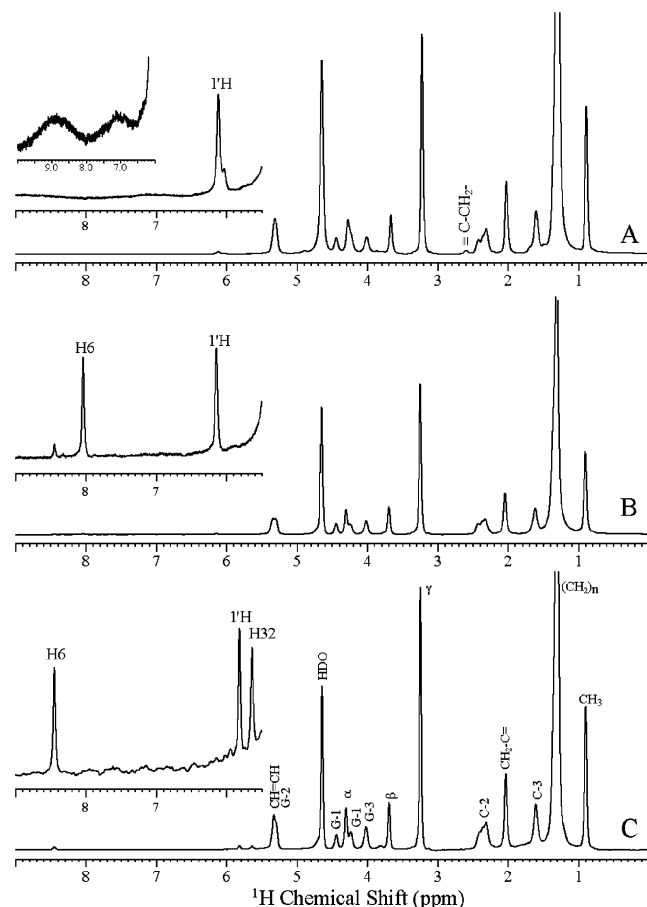


**Figure 5.**  $^1\text{H}$  MAS NMR spectra of 1/POPC (part A), 2/POPC (part B), and 3/POPC membranes (part C), all at a molar mixing ratio of 1:4, water content of 40 wt %, and MAS rotational frequency of 7 kHz. The assignment of the lipid peaks were taken from ref 61. The assignments of the resolved signals from the lipophilic nucleosides were obtained from HSQC spectra acquired in chloroform/methanol solution (1:1, v/v). The temperature of the measurement was 303 K. Insets show the enlarged downfield region of the spectra.

The plot of the cross-relaxation rates between a given segment of the lipophilic nucleosides and all POPC lipid segments provides a profile of the interaction strength between molecular segments along the molecular director of the lipid bilayer.<sup>43</sup> These plots are shown in Figure 7. The quantitative cross-peak analysis is rendered difficult by intramolecular contributions within the lipophilic nucleoside molecules. Therefore, the pattern of intramolecular NOEs of the nucleosides has been investigated in a perdeuterated DMPC- $d_{67}$  membrane. Because of the superposition of signals from the ribose of **1** and the POPC  $\beta$ -headgroup signal, these cross-peaks have been omitted from the analysis (indicated by an asterisk in Figure 7). Intramolecular cross-peaks between (deoxy)ribose or nucleobase signals with the lipid chains of the nucleosides are very weak or not present, as confirmed by NOESY measurements of the nucleosides in perdeuterated DMPC- $d_{67}$ .

The investigated segments of lipophilic nucleosides **1**, **2**, and **3** are broadly distributed along the director of the phospholipid membrane. Such broad distributions are also found for other small, membrane-associated molecules<sup>42,44–46</sup> and represent the thermal disorder of these liquid crystalline structures also observed by other methods.<sup>47–50</sup> Nevertheless, the highest cross-relaxation rates indicate high contact probabilities and, therefore, the most probable position of the respective molecular groups of the lipophilic nucleosides in the POPC membrane. If

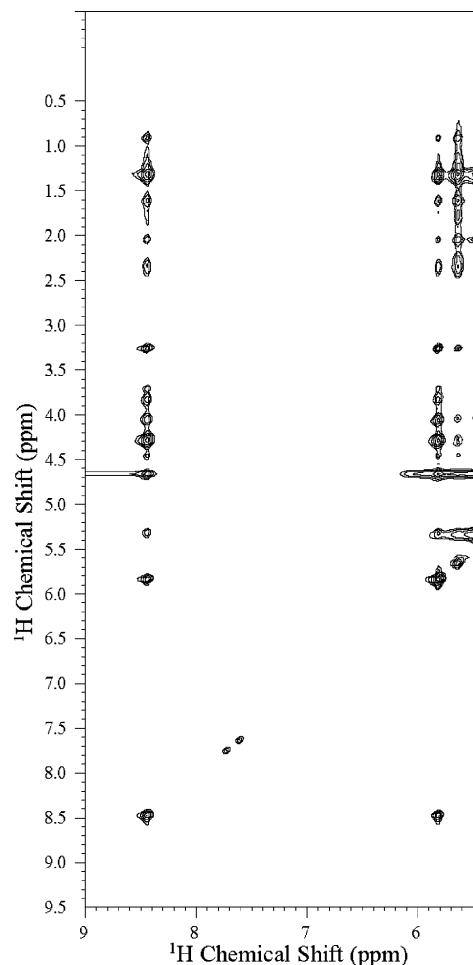


**Figure 6.** Contour plot of the downfield region of a  $^1\text{H}$  MAS NOESY spectrum of a 3/POPC mixture (1:4 molar ratio) at a mixing time of 300 ms, water content of 40 wt % and temperature of 303 K. All cross-peaks have positive intensity.

characteristic segments of a molecule can be resolved, the cross-relaxation rate profiles allow us to obtain the orientation of the molecule in the lipid membrane.<sup>44,51</sup>

For **1** (Figure 7 left), only the first methylene group of the acyl chain ( $\equiv\text{C}-\text{CH}_2-$ ) shows detectable cross-peaks with the upper lipid chain of POPC (Figure 7A), while the ribose  $1'$  H-atom exhibits a broad distribution with a clear maximum in the glycerol region of POPC (Figure 7B). This agrees with a localization of the adenine/ribose moiety in the lipid–water interface of the membrane, while the acyl chains are inserted in an analogous manner to the phospholipid chains.

For **2** (Figure 7 middle), cross-peaks of the uracil proton H6 and the deoxyribose  $1'$  H proton with the POPC molecules can be observed. Again, these segments are broadly distributed in the membrane with maxima of the distribution in the upper chain/glycerol region of the POPC membrane. These data suggest that **2** has a very similar membrane orientation to that of **1**.

For **3** (Figure 7 right), the cross-peaks of three protons with the lipid membrane are detectable. The H32 proton of the steroid ring of **3** has its maximum of the distribution function in the upper chain region of the POPC membrane and shows only very small cross-relaxation rates with the phospholipid headgroup (Figure 7E). The distribution functions of the uracil proton H6 (Figure 7F) and the ribose proton  $1'$  H (Figure 7G) exhibit their maxima in the headgroup region of POPC. These data suggest a location of the uracil/ribose moiety of **3** in the lipid–water

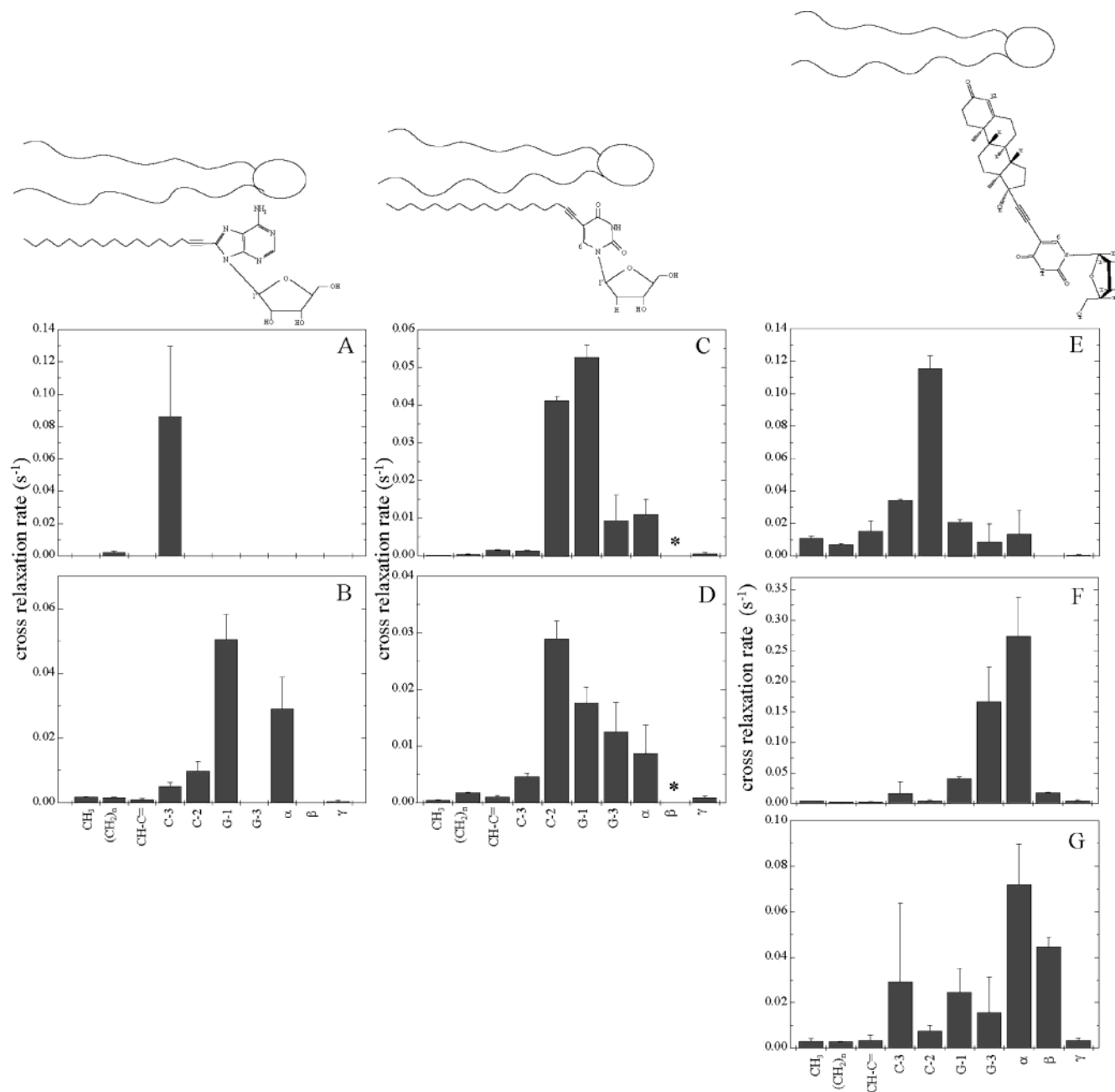


**Figure 7.** Cross-relaxation rates (s<sup>-1</sup>) between molecular segments of the lipophilic nucleosides and phospholipid segments from the POPC membrane. Left: **1** acyl chain≡C-CH<sub>2</sub>- (part A) and ribose 1' H (part B). Middle: **2** deoxyribose 1' H (part C) and uracil H6 (part D). Right: **3** steroid H32 (part E), ribose 1' H (part F), and uracil H6 (part G). The differences in the magnitudes of cross-relaxation rates between the different distribution profiles originate from small differences of the correlation times of motion, which modulate the magnetization transfer. Sketches of the approximate membrane location of the molecules are shown above. The asterisk (\*) indicates cross-relaxation rates that have not been included in the analysis because of significant intramolecular contributions. For numbering of positions of POPC, see Figure 1.

interface of the membrane. Also, the hydrogen atom in position 32 undergoes strong interactions with the upper chain region of the POPC membrane, indicating that the steroid moiety is only shallowly inserted.

## Discussion

In this study, the membrane incorporation of three different lipophilic nucleosides **1**, **2**, and **3** have been investigated with regard to nanobiotechnological applications. The main goal of this approach is to obtain structured and highly functional biological surfaces with recognition properties. Here, lipophilic nucleosides have been synthesized that are anchored in the membrane and exhibit a nucleobase moiety that is accessible

from the aqueous phase. These groups provide sites for hydrogen bonding with external molecular patterns such as single-stranded RNA or DNA, for instance via Watson-Crick base pairing. It is, therefore, important to obtain information about the membrane location and orientation of these membrane-associated nucleobases to assess if, for instance, steric or electric factors would interfere with the recognition patterns.

Several strategies for the synthesis of such membrane-anchored nucleosides are possible. We have chosen three different nucleobase monosaccharide moieties as hydrophilic groups that should exhibit a strong propensity toward the aqueous phase. A number of chemical structures can provide a lipophilic membrane anchor of the nucleosides. Particularly



appealing are the hydrocarbon chains that are also found in nature to anchor large proteins to membrane surfaces.<sup>18</sup> It has been shown that each methylene group of a lipid chain contributes  $\sim 0.8$  kcal/mol of hydrophobic energy.<sup>52</sup> Thus, substantial binding energy is accumulated for longer hydrocarbon chains. By using lipid chains of varying length, the strength of the hydrophobic interaction can be varied, and the anchoring of the nucleosides in the membrane is adapted to special applications. Alternatively, other hydrophobic molecular structures such as steroids can be used to create a lipophilic group that anchors the nucleosides to the membrane.

Though rationally designed, these molecules may not necessarily represent structures that are well suited for the desired purpose. For instance, lipophilic nucleosides could impose a positive curvature stress onto the membrane that would lead to membrane disruption or the formation of nonlamellar phases. Alternatively, lipophilic nucleosides could preferentially form micelles or exchange between a membrane-bound and a free state.<sup>12,53</sup> Such effects have, for instance, been observed for lipidated peptides that bind to the membrane by only one acyl chain.<sup>54–56</sup>

Therefore, we have studied the structure of the host membrane after incorporation of high concentrations of three newly synthesized lipophilic nucleosides with different membrane-anchoring groups, which were covalently linked by stable C–C bonds. Furthermore, the localization of the hydrophilic group in the membrane was determined.

All investigated lipophilic nucleosides **1**, **2**, and **3** incorporate well into POPC and DMPC membranes even at a high molar ratio of 20 mol %. The membrane structures maintained their lamellar liquid crystalline character, as detected by <sup>31</sup>P NMR. Insignificant alterations of the phospholipid headgroup orientation are observed in the <sup>2</sup>H NMR spectra. Only for **1**, somewhat broadened <sup>31</sup>P and <sup>2</sup>H NMR spectra of the membrane have been found. These broadenings could be related to an influence of **1** on the headgroup mobility of the phospholipids. This would be in agreement with the extreme broadening of the hydrogen at the C2-position of the adenine moiety in the <sup>1</sup>H MAS NMR spectra (Figure 5A). Several groups on the adenine/ribose segment, on one side, and the phospholipid headgroups and chain carbonyls of the membrane, on the other side, represent donors or acceptors for hydrogen bonding, which could influence the dynamics of both molecules.

Although the membrane incorporates and tolerates rather high concentrations of lipophilic nucleosides **1**, **2**, and **3**, the packing properties of the lipid acyl chains are influenced. The lowest effect is observed for **2**. This molecule has the smallest hydrophilic group and apparently fits best into the membrane. The hydrophilic group of **1** comprising an adenine instead of an uracil moiety is somewhat larger and, therefore, requires more space in the lipid–water interface of the membrane. As a consequence, the lipid molecules have to move apart laterally to allow the incorporation of this group. Consequently, the phospholipid chains experience more freedom of motion and decrease their order accordingly to allow motions of larger amplitude to take place. For **3**, the effect of phospholipid disordering is most significant even though it has the smaller headgroup consisting of the ribose/uracil moiety. The decrease in phospholipid order is particularly pronounced in the lower half of the chain (see inset of Figure 4). This result is first somewhat surprising, because natural steroids typically increase the molecular order in membranes.<sup>51,57–59</sup> Therefore, a somewhat different insertion of this molecular group is expected, compared to that of, for instance, cholesterol.

Besides the stable anchoring of lipophilic nucleosides in membranes, the exposition of the nucleobase in the aqueous phase is important for the recognition and binding to external patterns. If this part of the molecule is not sufficiently hydrophilic, it will be buried in the membrane and resist binding to the external complementary DNA patterns. Therefore, we studied the localization of the nucleobases and (deoxy)ribose moieties with respect to the lipid membranes by <sup>1</sup>H MAS NOESY NMR.

As expected, for all lipophilic nucleosides, a preferential localization in the glycerol/headgroup region of the membrane has been found. Because of the accumulation of hydrophilic functional groups, these molecular segments exhibit a propensity for the more polar environment. In the lipid–water interface, the hydroxyl, carbonyl, and amino groups of the nucleobases and the monosaccharides can form hydrogen bonds with the respective groups of the lipid carbonyl and phosphate groups. Furthermore, electrostatic forces by dipole–charge or dipole–dipole interactions can stabilize these groups in the membrane interface, establishing a structure of lowest free energy. However, the structure is highly dynamic and best described by a several angstroms broad distribution in the *z* direction.<sup>46</sup> This is a consequence of the roughness of the membrane surface and the high mobility of the molecules in a liquid crystalline membrane that even allow for head-to-tail contacts.<sup>60</sup> Regardless, the molecules maintain their average structure and, thus, expose the nucleobase moiety toward the aqueous phase.

For nucleoside **3**, the membrane insertion is somewhat different from that of lipidated nucleoside **1** or **2**. The ring hydrogen at position 32 is localized in the upper chain region of the phospholipid bilayer. This is explained by the neighborhood to the polar carbonyl group in position 33. This group has a propensity for the more polar lipid–water interface of the membrane and hampers the insertion of the steroid ring system. Therefore, the molecule only shallowly penetrates the membrane. This explains the significant order decrease of the lower phospholipid chain segments observed by <sup>2</sup>H NMR (see inset in Figure 4). **3** is bound in the lipid–water interface of the membrane and does not penetrate the membrane core. Therefore, the molecule may act as a spacer in the glycerol/upper chain part pushing apart the phospholipids laterally. This creates free volume in the lower part of the phospholipid chains, which is occupied by the larger amplitudes of motions indicated by lower order parameters of the phospholipid chains.

## Conclusion

We have synthesized three different lipophilic nucleosides and investigated their membrane insertion and localization. All molecules can be incorporated into phospholipid membranes at high concentration without destroying the bilayer structure or the formation of nonlamellar phases. Insignificant alterations of the phospholipid headgroup structure have been observed with the exception of nucleoside **1**. Nucleosides with a lipid alkynyl chain membrane anchor only slightly influence the packing properties of the membrane. However, **3**, bearing a steroidal ring system as the lipophilic group, significantly decreases lipid order parameters and decreases the packing density in the membrane. For all molecules, an interface location of the (deoxy)ribose/nucleobase moiety has been found that exposes the nucleobase to the aqueous phase, where an interaction with external molecular patterns can take place. From the current study, we judge that **2** has the most promising properties for the structuring and functionalization of lipid surfaces, because it (i) does not influence or interact with the



phospholipid headgroups, (ii) only very insignificantly influences the chain packing of the host matrix, and (iii) exposes the uracil moiety to the aqueous phase. Next, it needs to be demonstrated that single-stranded DNA can bind to several lipophilic nucleosides in the membrane by multiple interactions to create thermodynamically stable nanostructures. These experiments are currently underway in our laboratories.

**Acknowledgment.** The study was supported by a grant by the Bundesministerium für Bildung und Forschung. W.F. wants to thank Schering AG for a generous grant. Financial support by Fonds der Chemischen Industrie is gratefully acknowledged.

## References and Notes

- (1) Mirkin, C. A.; Letsinger, R. L.; Mucic, R. C.; Storhoff, J. J. *Nature* **1996**, *382*, 607–609.
- (2) Mirkin, C. A. *Inorg. Chem.* **2000**, *39*, 2258–2272.
- (3) Niemeyer, C. M. *Trends Biotechnol.* **2002**, *20*, 395–401.
- (4) Niemeyer, C. M. *Angew. Chem., Int. Ed.* **2001**, *40*, 4128–4158.
- (5) Goodsell, D. S. *Bionanotechnology*; John Wiley & Sons: Hoboken, NJ, 2004.
- (6) Niemeyer, C. M. *Curr. Opin. Chem. Biol.* **2000**, *4*, 609–618.
- (7) Yoshina-Ishii, C.; Boxer, S. G. *J. Am. Chem. Soc.* **2003**, *125*, 3696–3697.
- (8) Moreau, L.; Barthelemy, P.; El Maataoui, M.; Grinstaff, M. W. *J. Am. Chem. Soc.* **2004**, *126*, 7533–7539.
- (9) Kurihara, K.; Abe, T.; Nakashima, N. *Langmuir* **1996**, *12*, 4053–4056.
- (10) Pincet, F.; Perez, E.; Bryant, G.; Lebeau, L.; Mioskowski, C. *Phys. Rev. Lett.* **1994**, *73*, 2780–2783.
- (11) Marlow, A. L.; Mezzina, E.; Spada, G. P.; Masiero, S.; Davis, J. T.; Gottarelli, G. *J. Org. Chem.* **1999**, *64*, 5116–5123.
- (12) Gosse, C.; Boutorine, A.; Aujard, I.; Chami, M.; Kononov, A.; Cogné-Laage, E.; Allemand, J.-F.; Li, J.; Jullien, L. *J. Phys. Chem. B* **2004**, *108*, 6485–6497.
- (13) Iwaura, R.; Yoshida, K.; Masuda, M.; Ohnishi-Kameyama, M.; Yoshida, M.; Shimizu, T. *Angew. Chem., Int. Ed.* **2003**, *42*, 1009–1012.
- (14) Paterson, I.; Man, J. *Tetrahedron Lett.* **1997**, *38*, 691–694.
- (15) Manoharan, M.; Tivel, K. L.; Cook, P. D. *Tetrahedron Lett.* **1995**, *36*, 3651–3654.
- (16) MacKellar, C.; Graham, D.; Will, D. W.; Burgess, S.; Brown, T. *Nucleic Acids Res.* **1992**, *20*, 3411–3417.
- (17) Boutorin, A. S.; Gus'kova, L. V.; Ivanova, E. M.; Kobetz, N. D.; Zarytova, V. F.; Rytte, A. S.; Yurchenko, L. V.; Vlassov, V. V. *FEBS Lett.* **1989**, *254*, 129–132.
- (18) Casey, P. J. *Science* **1995**, *268*, 221–225.
- (19) Schafer, W. R.; Rine, J. *Annu. Rev. Genet.* **1992**, *26*, 209–237.
- (20) Berti, D.; Franchi, L.; Baglioni, P. *Langmuir* **1997**, *13*, 3438–3444.
- (21) Pincet, F.; Lebeau, L.; Cribier, S. *Eur. Biophys. J.* **2001**, *30*, 91–97.
- (22) Pincet, F.; Rawicz, W.; Perez, E.; Lebeau, L.; Mioskowski, C.; Evans, E. *Phys. Rev. Lett.* **1997**, *79*, 1949–1952.
- (23) Cullis, P. R.; de Kruijff, B. *Biochim. Biophys. Acta* **1979**, *559*, 399–420.
- (24) Davis, J. H. *Biochim. Biophys. Acta* **1983**, *737*, 117–171.
- (25) Seelig, J. *Q. Rev. Biophys.* **1977**, *10*, 353–418.
- (26) Scherer, P. G.; Seelig, J. *Biochemistry* **1989**, *28*, 7720–7728.
- (27) Huster, D.; Gawrisch, K. New insights into biomembrane structure from two-dimensional nuclear Overhauser enhancement spectroscopy. In *Lipid bilayers: structure and interactions*; Katsaras, J., Gutberlet, T., Eds.; Springer-Verlag: Berlin, 2000; pp 109–125.
- (28) Flasche, W.; Cismas, C.; Herrmann, A.; Liebscher, J. *Synthesis*, in press.
- (29) Kay, L. E.; Keifer, P.; Saarinen, T. *J. Am. Chem. Soc.* **1992**, *114*, 10663–10665.
- (30) Davis, J. H.; Jeffrey, K. R.; Bloom, M.; Valic, M. I.; Higgs, T. P. *Chem. Phys. Lett.* **1976**, *42*, 390–394.
- (31) Huster, D.; Arnold, K.; Gawrisch, K. *Biochemistry* **1998**, *37*, 17299–17308.
- (32) McCabe, M. A.; Wassall, S. R. *J. Magn. Reson., Ser. B* **1995**, *106*, 80–82.
- (33) Lafleur, M.; Fine, B.; Sternin, E.; Cullis, P. R.; Bloom, M. *Biophys. J.* **1989**, *56*, 1037–1041.
- (34) Nagle, J. F. *Biophys. J.* **1993**, *64*, 1476–1481.
- (35) Huster, D.; Dietrich, U.; Gutberlet, T.; Gawrisch, K.; Arnold, K. *Langmuir* **2000**, *16*, 9225–9232.
- (36) Katsaras, J.; Jeffrey, K. R.; Yang, D. S.; Epand, R. M. *Biochemistry* **1993**, *32*, 10700–10707.
- (37) Jeener, J.; Meier, B. H.; Bachmann, P.; Ernst, R. R. *J. Chem. Phys.* **1979**, *71*, 4546–4553.
- (38) Wagner, G.; Wüthrich, K. *J. Mol. Biol.* **1982**, *155*, 347–366.
- (39) Macura, S.; Ernst, R. R. *Mol. Phys.* **1980**, *41*, 95–117.
- (40) Huster, D.; Arnold, K.; Gawrisch, K. *J. Phys. Chem. B* **1999**, *103*, 243–251.
- (41) Feller, S. E.; Huster, D.; Gawrisch, K. *J. Am. Chem. Soc.* **1999**, *121*, 8963–8964.
- (42) Feller, S. E.; Brown, C. A.; Nizza, D. T.; Gawrisch, K. *Biophys. J.* **2002**, *82*, 1396–1404.
- (43) Holte, L. L.; Gawrisch, K. *Biochemistry* **1997**, *36*, 4669–4674.
- (44) Scheidt, H. A.; Pampel, A.; Nissler, L.; Gebhardt, R.; Huster, D. *Biochim. Biophys. Acta* **2004**, *1663*, 97–107.
- (45) Huster, D.; Müller, P.; Arnold, K.; Herrmann, A. *Biophys. J.* **2001**, *80*, 822–831.
- (46) Yau, W. M.; Wimley, W. C.; Gawrisch, K.; White, S. H. *Biochemistry* **1998**, *37*, 14713–14718.
- (47) Wiener, M. C.; White, S. H. *Biophys. J.* **1992**, *61*, 434–447.
- (48) White, S. H.; Wiener, M. C. The liquid-crystallographic structure of fluid lipid bilayer membranes. In *Biological membranes. A molecular perspective from computation and experiment*; Merz, K. M., Roux, B., Eds.; Birkhäuser: Boston, 1996; pp 127–144.
- (49) Petrache, H. I.; Gouliav, N.; Tristram-Nagle, S.; Zhang, R.; Suter, R. M.; Nagle, J. F. *Phys. Rev. E: Stat. Phys., Plasmas, Fluids, Relat. Interdiscip. Top.* **1998**, *57*, 7014–7024.
- (50) Venable, R. M.; Zhang, Y.; Hardy, B. J.; Pastor, R. W. *Science* **1993**, *262*, 223–226.
- (51) Scheidt, H. A.; Müller, P.; Herrmann, A.; Huster, D. *J. Biol. Chem.* **2003**, *278*, 45563–45569.
- (52) Tanford, C. *The hydrophobic effect: formation of micells and biological membranes*; John Wiley & Sons: New York, 1980.
- (53) Zandomenighi, G.; Luisi, P. L.; Mannina, L.; Segre, A. *Helv. Chim. Acta* **2001**, *84*, 3710–3725.
- (54) Heerklotz, H.; Wieprecht, T.; Seelig, J. *J. Phys. Chem. B* **2004**, *108*, 4909–4915.
- (55) Peitzsch, R. M.; McLaughlin, S. *Biochemistry* **1993**, *32*, 10436–10443.
- (56) Shahinian, S.; Silvius, J. R. *Biochemistry* **1995**, *34*, 3813–3822.
- (57) Oldfield, E.; Meadows, M.; Rice, D.; Jacobs, R. *Biochemistry* **1978**, *17*, 2727–2740.
- (58) Urbina, J. A.; Pekarar, S.; Le, H. B.; Patterson, J.; Montez, B.; Oldfield, E. *Biochim. Biophys. Acta* **1995**, *1238*, 163–176.
- (59) Krajewski-Bertrand, M.-A.; Milon, A.; Hartmann, M.-A. *Chem. Phys. Lipids* **1992**, *63*, 235–241.
- (60) Huster, D.; Gawrisch, K. *J. Am. Chem. Soc.* **1999**, *121*, 1992–1993.
- (61) Volke, F.; Pampel, A. *Biophys. J.* **1995**, *68*, 1960–1965.